New Functions of Polyolefin for Manipulated Iron Oxide Nanostructure Synthesis

Qingliang He*, Suying Wei** and Zhanhu Guo*

* Integrated Composites Laboratory (ICL), Dan F. Smith Department of Chemical Engineering, Lamar University, Beaumont, Texas 77710 USA, qhe@lamar.edu, zhanhu.guo@lamar.edu
** [b]Department of Chemistry and Biochemistry, Lamar University, Beaumont, Texas 77710 USA, suying.wei@lamar.edu

ABSTRACT

An old-fashioned polypropylene (PP) grafted maleic anhydride, denoted as PP-g-MA, was sucessfully utilized to serve as polymeric surfactant to synthesize stable magnetic nanoparticles (NPs) through a facile one-pot bottom up method. To be specific, through thermal decomposing organometallic precursor, $Fe(CO)_5$/$Co_2(CO)_8$ in refluxing PP-g-MA–solvent, or PP–PP-g-MA–xylene: 1.) PP-g-MA (M_n≈ 8000 g/mol) with different concentration exhibited simutaneously control over the morphologies (hollow NPs vs. chain-like nanostructures), crystalline phases (α- vs. γ-phase) and magnetic properties (super-paramagnetic vs. hard ferromagnetic) in synthesizing Fe_2O_3 NPs; 2.) PP-g-MAs with different backbone chain-lengths (M_n≈ 2500, and 800 g/mol) were demonstrated in controlling the cobalt morphologies (dispersed polyhedral vs. self-assembled nanchian structure), crystalline phases (ε- vs. β- phase), and magnetic property (242 vs. 808 Oe coercivity) in the synthesized magnetic PP nanocomposites.

Keywords: magnetic, iron oxide, nanoparticles, surfactant, polypropylene grafted maleic anhydride

Introduction

Magnetic nanoparticles (NPs) and their reinforced polymer nanocomposites (PNCs) have been extensively studied due to their unique physicochemical properties and potential technological applications such as electric sonsor devices, electromagnetic shielding, information storage, magnetic resonance imaging, and magnetic field directed drug delivery. Meanwhile, the magnetic properties have been considered to be strongly related to the particle size, morphology, crystalline structure and et al.[1] Extensive efforts have been made to design magnetic nanomaterials, which can effectively control these aforementioned parameters in order to target desirable multi-functionalities. In iron group, due to the rich crystalline phase structures of iron oxide (α-, β-, γ- and ε-), metal cobalt (α-, β-, and ε-), there are strong needs for developing a general approach to control the crystal phase of iron oxides and cobalt NPs. Among developed approaches for synthesizing magnetic NPs such as high temperature reduction of iron/cobalt salts, melting crystallization, evaporation condensation, and thermal decomposition of neutral organometal precursor, the relative low temperature solution chemistry is usually ideal for yielding exclusively one crystal structure magnetic NPs.[2] In addition, the aids of surfactants and stabilizers are essential to produce highly dispersed magnetic NPs due to their tendency for agglomerations because of the intrinsic strong magnetic dipolar and Van der Waals forces.

Functional polymers/copolymers with polar structures in their backbones[3-7] are ideal for serving as the hosting matrices for magnetic NPs. However, inert polymer such as PP has rarely been reported to serve as matrix to synthesize magnetic NPs or magnetic PP PNCs. Because the lack of strong interaction between the PP matrix and the magnetic NPs will cause poor coordiantions for these NPs and deteriorated performances. On the other hand, a long known cost effective polymeric additive, PP-g-MA has potential to serve as surfactant to these magnetic NPs due to handful reports on its excellent compatibilizing/coupling effects. [8-12] Meanwhile, the scarcity of reporting its surfactant effect stimulate the unearth of how PP-g-MA can act in synthesizing magnetic NPs. Here, three PP-g-MAs with different molecular weights was utilized to synthesize iron oxide and cobalt NPs using a one-pot bottom up method. TEM (Transmission electron microscopy) and XRD (X-ray diffraction) were used to characterize the morphology and crystalline structure of thus syntheiszed NPs. In addition, room temperature magnetic property was also studied.

Materials

Isotactic PP used was supplied by Total Petrochemicals USA, Inc (ρ=0.9 g/cm^3, M_n≈40500). PP-g-MAs with three different molecular weights (1. M_n≈8000; 2. M_n≈2500; 3. M_n≈800) was provided by Baker Hughes. PP-g-MA-1 (M_n≈8000) is a homo-PP with one terminal MA through Alder-ENE reaction and one additional MA grafting; PP-g-MA-2 (M_n≈2500) is a homo-PP with one terminal MA through Alder-ENE reaction; and PP-g-MA-3 (M_n≈800) is a propylene-hexene copolymer with one MA at one terminal and the other MA grafted on the main chain. Iron(0) pentacarbonyl ($Fe(CO)_5$, 99%) was commercially obtained from Sigma Aldrich. Dicobalt octacarbonyl ($Co_2(CO)_8$, stabilized with 1-5% hexane) was obtained from Strem Chemicals, Inc. Solvent xylene (laboratory grade, ρ=0.87 g/cm^3) was purchased from Fisher Scientific. All the

chemicals were used as-received without any further treatment.

Experimental Section

Typical synthesis of Fe_2O_3 NPs were described as below: 1st, specific amount PP-g-MA-1 and 100 ml xylene were added into a 250 ml three-neck flask and heated to reflux with at 140 °C constant. A homogeneous solution was formed upon the total dissolution of PP-g-MA in xylene after refluxing at 140 °C for 30 min. 2nd, cool the solution to ~ 120 °C for 5 min; then, a calculated amounts of $Fe(CO)_5$ was injected into the hot solution. The solution turned to yellow; then became a black colloidal solution upon additional 3-h refluxing at 140 °C. After cooling to room temperature (RT), the black solution was transferred to a glass container to slowly evaporate xylene in the fume hood. Finally, the received black products were dried in the vacuum oven (RT) for 24 h to form the final composites. The weight ratios between PP-g-MA-1 and iron (from $Fe(CO)_5$) here are 1:1 and 1:4. For synthesizing PP/Co PNCs: 1st, 7.5 g PP pellets, 0.5 g PP-g-MA-2 (or -3) and 100 ml xylene were added into a 500 ml three-neck flask; then heated the mixture (at ~140 °C) to dissolve the polymers while keep mechanic stirring at 200 rpm. 2nd, the solution was cooled down to ~ 110-120 °C; meanwhile, 5.8 g $Co_2(CO)_8$ was dissolved in 120~130 ml xylene in glove box. 3rd, the freshly prepared $Co_2(CO)_8$/xylene solution was injected into the flask to obtain 20% Co in PP/PP-g-MA. (Calculation was based on the pure cobalt weight fraction). Keep stirring at 200 rpm and heating at 140 °C constant, the solution turned from transparent to brown, then became black during an additional 3-h refluxing. Finally, the PNCs was collected by the same procedures as aforemetioned for Fe_2O_3 NPs. PP/20.0 wt% Co PNCs was also synthesized for comparison (8.0g PP and 5.8 g $Co_2(CO)_8$).

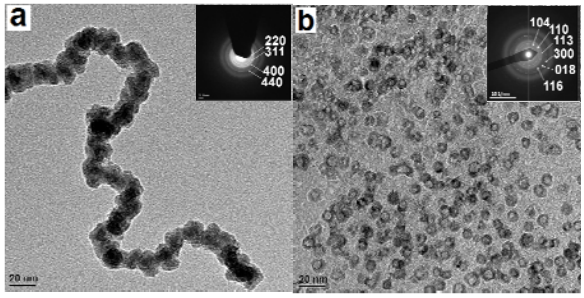

Figure 1 TEM of a) γ-Fe_2O_3 nanochain (PP-g-MA-1: Fe =1:4); and b) α-Fe_2O_3 hollow NPs (PP-g-MA-1: Fe=1:1)

Characterization

The NP morphology of the as prepared samples was investigated using TEM in a FEI TECNAI G2 F20 microscope at a working voltage of 200 kV. Typically, one droplet of the diluted colloid solution was dropped onto carbon-film coated copper grids to form a TEM specimen upon evaporation of the solvent. The selected area electron diffraction (SAED) patterns were taken using a large selected-area aperture and recorded by a Gatan SC1000 ORIUS CCD camera. The magnetic property measurements were carried out in a 9 T physical properties measurement system (PPMS) by Quantum Design.

Results and Discussion

Morphology and Crystalline Structure

Fig. 1 a&b demonstrated the TEM images of Fe_2O_3 NPs with different morphology formed through using different PP-g-MA-1 (M_n≈8000) concentration in thermal decomposing $Fe(CO)_5$ in refluxing PP-g-MA-1/xylene. As shown in Fig. 1a, by using a low PP-g-MA-1 concentration (PP-g-MA:Fe= 1:4), self assembled chain-like structures with average individual particle size of ~20 nm was observed from drop-casting the as-prepared colloid onto a copper grid. All the ring patterns in SAED can be assigned to γ-Fe_2O_3 (insert of Fig. 1a). When increasing PP-g-MA-1 concentration (PP-g-MA:Fe = 1:1), mono-dispersed NPs (diameter at 7.7±1.0 nm) were observed through the same reaction condition, Figure 1b. In addition, the as-prepared NPs exhibited hollow structure; meanwhile, SAED patterns (insert of Fig. 1b) can be assigned to α-Fe_2O_3.

Upon heating, $Fe(CO)_5$ was decomposed to form metallic iron nuclei with releasing CO, then the iron NPs were formed upon the growth of these iron nuclei when its concentration reached a critical threshold. Simutaneously, oxidization took place on the surface of iron NPs under open air synthesis condition and an oxide layer formed on the iron NPs' surface. Carboxylic groups formed from the hydrolysis of MA groups can bound on the oxide surface and the growth of the NPs can thus be restricted.[13] In addition, oxygen further penetrated and diffused to the metal core and formed more oxide due to the high reactivity of nanosized iron. Meanwhile, a outward diffusion of iron took place. With reaction proceeded further, the outward diffusion of iron through the oxide layer became faster than the inward oxygen diffusion, and the iron core was gradually consumed with shrinking core size until the core is completely depleted. Finally, after 3-h reaction under air, the hollow structure Fe_2O_3 NPs were formed upon a total consumption of the iron core through the nano-scale Kirkendall effect.[14]

When decreasing PP-g-MA concentration, the formed particle size was enlarged with relatively more available iron nuclei and less amount of PP-g-MA presented in the xylene solution. Nonetheless, the repulsion forces derived from the steric hindrance of the bonded PP-g-MA backbone on these NPs were not strong enough to repulse these NPs separately,which is due to the existence of stronger magnetic dipolar-dipolar interactions among these magnetic NPs. Hence, these NPs self assembled into nanochain structure.[15] The morphology of Fe_2O_3 NPs are usually reported to be controlled by varying synthesis condition commonly, however, the simutaneously control over the crystalline structures of Fe_2O_3 NPs is rarely been reported.

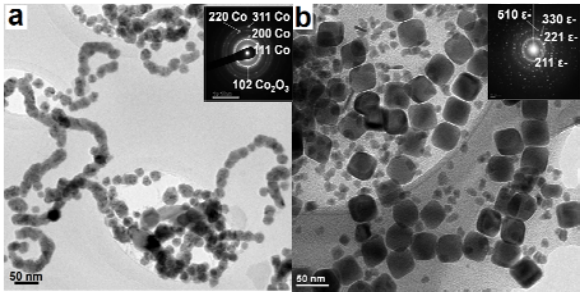

Figure 2 TEM images of a) fcc-cobalt NPs formed in PP/20.0% Co PNCs with 5.0% PP-g-MA-2; and b) ε-cobalt NPs formed inPP/20.0% Co PNCs with 5.0% PP-g-MA-3.

Fig. 2 a&b showed the TEM images of the PP-20.0% Co-5.0% PP-g-MA-2 (M_n≈2500) PNCs, and PP-20.0 % Co -5.0% PP-g-MA-3 (M_n≈800) PNCs; respectively. When 5.0 % PP-g-MA (M_n≈2500) was incorporated into PP-20% Co system, the thus formed Co NPs (Fig. 2a) were observed to be assembled into a combination of Co chain-like structure and individual NPs with an average particle size of ~22 nm. The strong ring patterns in SAED (insert of Fig. 2a) can be assigned to the (111), (200), (220), and (311) planes of fcc-Co (PDF# 15-0806). Meanwhile, another ring pattern overlapped with the (111) plane of fcc-Co can be assigned to (102) plane of Co_2O_3 (PDF# 02-0770). It can thus concluded that the fcc-Co NPs are covered with a Co_2O_3 layer on its surface. With adding another PP-g-MA-3 (M_n≈800) into PP- 20.0% Co system, TEM image (Fig. 2b) demonstrated that separate polyhedral Co NPs (edge length: ~ 41 nm) including hexagonal, rhombic, and cubic shapes has formed. In addition, SAED patterns (insert of Fig. 2b) can be assigned to ε-phase cobalt. Thus, it is obvious that the morphology and crystalline phase of Co NPs can be also controlled simultaneously by varying the alkyl chain length of PP-g-MAwhile keep the same PP-g-MA concentration. The short PP-g-MA chains give more bonding density on the surface of Co NPs, which may cuase the formation of the dispersed large polyhedral NPs.

Magnetic Properties

Room temperature magnetic property revealed that PP-g-MA PNCs with hollow Fe_2O_3 NPs did not reach a saturation value within the applied 30 kOe external magnetic field (Fig. 3a), and the magnetization value was 2.9 emu/g at 30 kOe, which supported the formation of α-phase Fe_2O_3.[16-18] Moreover, there was no magnetic hysteresis loop, reflected the characteristic superpara-magnetic behavior of these hollow α- Fe_2O_3 NPs. However, PP-g-MA PNCs with Fe_2O_3 chain-like nanostructures showed a clear magnetic hysteresis loop and strong saturation magnetization (M_s) of 54.0 emu/g (Fig. 3b) as well as coercivity (H_c) of 518.0 Oe.This indicated a hard ferromagnetic behavior (Materials with Hc greater than 200 Oe is defined as hard ferromagnetic; and soft ferromagnetic has H_c smaller than 200 Oe).[19, 20]

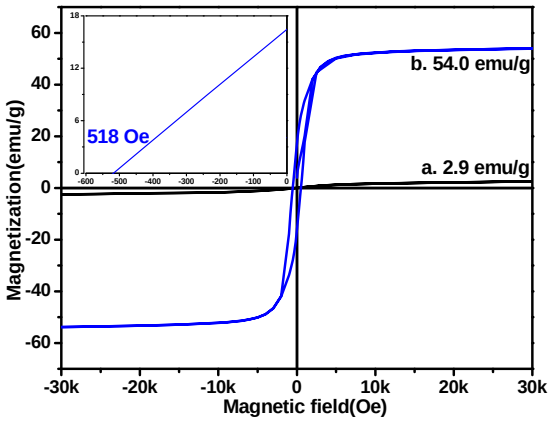

Figure 3 Room temperature hysteresis loops of the PP-g-MA-1PNCs with: a). hollow NPs and b). nanochains.

Fig. 4 further depicts room temperature hysteresis loops of the as-prepared PP/Co PNCs in the presence of PP-g-MA-2 and 3. When 5.0 % PP-g-MA-2 (M_n≈2500) was incorporated into PP-20% Co system, The M_s was 22.8 emu/g (~109.0 emu/g Co) with a H_c of 808 Oe, indicating a hard ferromagnetic behavior (Fig. 4a). When adding another 5.0 % PP-g-MA-3 (M_n≈800) into PP-20% Co system, The M_s was increased to 25.2 emu/g (~114.0 emu/g Co) with a significantly decreased H_c of 242 Oe (Fig. 4b). The high H_c of PP-5% PP-g-MA-2 (Mn≈2500) -20.0% Co sample are attributed to strong shape anisotropy from these chain-like nanostructures formed by fcc-Co NPs and exchange anisotropy generated between the ferro-magnetic Co core and the anti-ferromagnetic cobalt oxide shell.[21] Meanwhile, the relatively small H_c of PP-20.0% Co sample with 5% PP-g-MA-3 (Mn≈800) was primarily attibuted to exchange anisotropy between Co core and Co_2O_3 shell with minor effect from shape anisotropy due to the lack of chain-like nanostructures.

The M_s of both PP-Co PNCs was found to be lower than that of bulk Co (~162 emu/g) when converting the composite into pure Co species, also indicating the existence of anti-ferromagnetic cobalt oxide layer formed on the surface of the Co NPs. However, the increased magnetization in the presence of PP-g-MA-3 suggests that the more chemical bondings took place between the MA groups and the cobalt oxide layer when PP-g-MA molecular weight was decreased. Compared with PP-g-MA-2, the low molecular weight PP-g-MA-3 owns more MA groups at the same loading in final PP PNCs, which gives higher bonding density and leads to a higher stability of the thus formed Co NPs against oxidation.[22] So that the Co surface can be passivated with less oxide formation, and increase M_s can be achieved due to the enhanced the anti-oxidization strength. This is also consistent with our recent observation in Fe NPs.[23]

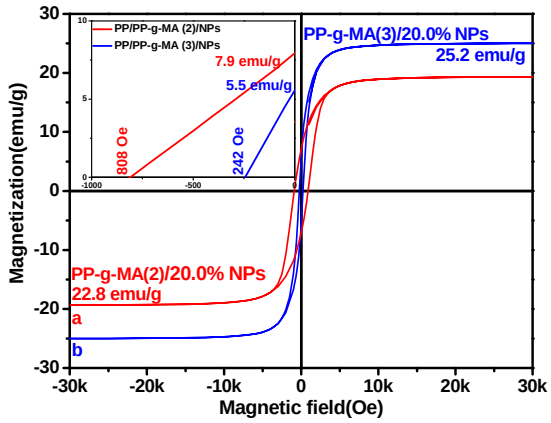

Figure 4 Room temperature hysteresis loops of the PP/(PP-g-MA)/Co NPs PNCs with: a) 5.0% PP-g-MA-2; and b) 5.0% PP-g-MA-3.

Conclusion

A new function of PP-g-MA acted as surfactant and stabilizer to synthesize stable magnetic Fe_2O_3 and Co NPs was successfully demonstrated. Either the PP-g-MA concentration or PP-g-MA backbone chain length played crucial roles in simultaneously manipulating the morphology and crystalline structure of the corresponding magnetic NPs in a conveninent way. The merits of the facile bottom up wet chemistry method utilized in this work including low-temperature, large-scale, one-pot route and structure compatibility with many kinds of polyolefin-based polymers and copolymers will broaden the utilization of PP-g-MA in preparing magnetic PNCs for a varierty of applications.

Acknowledgement

This project is supported by National Science Foundation-Chemical and Biological Separations (EAGER: CBET 11-37441); and Nanoscale Interdisciplinary Research Team and Materials Processing and Manufacturing (CMMI 10-30755). We also appreciate the Baker Hughes Inc. for partial financial support.

REFERENCES

[1] S. Wei, Q. Wang, J. Zhu, L. Sun, H. Lin, and Z. Guo, *Nanoscale,* vol. 3, pp. 4474-4502, 2011.

[2] D. P. Dinega and M. G. Bawendi, *Angew. Chem. Int. Ed.,* vol. 38, pp. 1788-1791, 1999.

[3] Z. Guo, L. L. Henry, V. Palshin, and E. J. Podlaha, *J. Mater. Chem.,* vol. 16, pp. 1772-1777, 2006.

[4] M. A. Zalich, V. V. Baranauskas, J. S. Riffle, M. Saunders, and T. G. S. Pierre, *Chem.Mater.,* vol. 18, pp. 2648-2655, 2006.

[5] X. H. Zhang, K. M. Ho, A. H. Wu, K. H. Wong, and P. Li, *Langmuir,* vol. 26, pp. 6009-6014, 2010.

[6] G. Liu, X. Yan, Z. Lu, S. A. Curda, and J. Lal, *Chem.Mater.,* vol. 17, pp. 4985-4991, 2005.

[7] L. A. Mîinea, B. Laura, K. D. Ericson, D. S. Glueck, and R. B. Grubbs, *Macromolecules,* vol. 37, pp. 8967-8972, 2004.

[8] S. Morlat, B. Mailhot, D. Gonzalez, and J. L. Gardette, *Chem.Mater.,* vol. 16, pp. 377-383, 2004.

[9] G. Galgali, C. Ramesh, and A. Lele, *Macromolecules,* vol. 34, pp. 852-858, 2001.

[10] P. J. Purohit, J. E. Huacuja-Sánchez, D. Y. Wang, F. Emmerling, A. Thünemann, G. Heinrich, and A. Schönhals, *Macromolecules,* vol. 44, pp. 4342-4354, 2011.

[11] H. Yu, Z. Zhang, Z. Wang, Z. Jiang, J. Liu, L. Wang, D. Wan, and T. Tang, *J. Phys. Chem. C,* vol. 114, pp. 13226-13233, 2010.

[12] M. C. Hsiao, S. H. Liao, Y. F. Lin, C. C. Weng, H. M. Tsai, C. C. M. Ma, S. H. Lee, M. Y. Yen, and P. I. Liu, *Energy Environ. Sci.,* vol. 4, pp. 543-550, 2011.

[13] Q. He, T. Yuan, S. Wei, N. Haldolaarachchige, Z. Luo, D. P. Young, A. Khasanov, and Z. Guo, *Angew. Chem. Int. Ed.,* vol. 51, pp. 8842-8845, 2012.

[14] Y. Yin, R. M. Rioux, C. K. Erdonmez, S. Hughes, G. A. Somorjai, and A. P. Alivisatos, *Science,* vol. 304, pp. 711-714, 2004.

[15] P. Y. Keng, I. Shim, B. D. Korth, J. F. Douglas, and J. Pyun, *ACS Nano,* vol. 1, pp. 279-292, 2007.

[16] X. Qu, N. Kobayashi, and T. Komatsu, *ACS Nano,* vol. 4, pp. 1732-1738, 2010.

[17] S. Zeng, K. Tang, T. Li, Z. Liang, D. Wang, Y. Wang, Y. Qi, and W. Zhou, *J. Phys. Chem. C,* vol. 112, pp. 4836-4843, 2008.

[18] K. T. Van, H. G. Cha, K. C. Nguyen, S. W. Kim, M. H. Jung, and Y. S. Kang, *Cryst. Growth Des.,* vol. 12, pp. 862-868, 2012.

[19] Q. He, T. Yuan, J. Zhu, Z. Luo, N. Haldolaarachchige, L. Sun, A. Khasanov, Y. Li, D. P. Young, and S. Wei, Zhanhu Guo, *Polymer,* vol. 53, pp. 3642–3652 2012.

[20] Q. He, T. Yuan, Z. Luo, N. Haldolaarachchige, D. P. Young, S. Wei, and Z. Guo, *Chem. Comm,* vol. 49, pp. 2679-2681, 2013.

[21] D. Srikala, V. Singh, A. Banerjee, B. Mehta, and S. Patnaik, *J. Phys. Chem. C,* vol. 112, pp. 13882-13885, 2008.

[22] R. M. de Silva, V. Palshin, F. R. Fronczek, J. Hormes, and C. S. S. R. Kumar, *J. Phys. Chem. C,* vol. 111, pp. 10320-10328, 2007.

[23] J. Zhu, Q. He, Z. Luo, A. Khasanov, Y. Li, L. Sun, Q. Wang, S. Wei, and Z. Guo, *J. Mater. Chem.,* vol. 22, pp. 15928 -15938, 2012.